University of Arizona | Carnegie Institution of Washington | The Johns Hopkins University

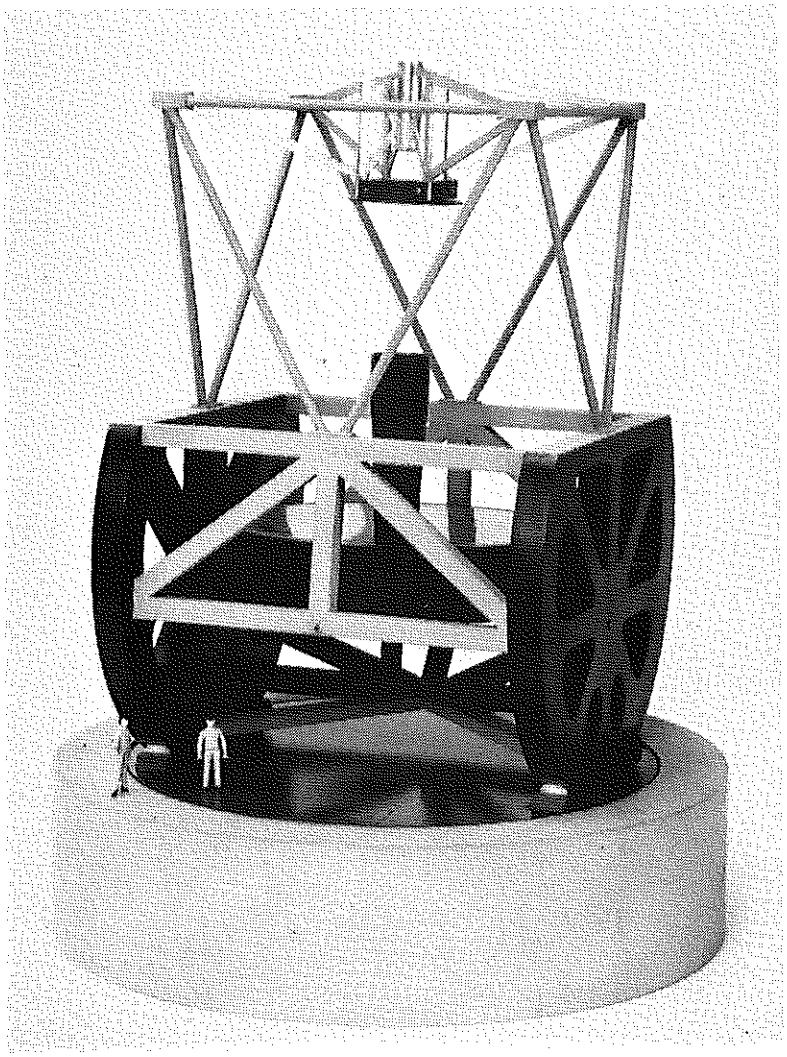

Diffraction Analysis at the Wide-Field Infrared Focus of the Columbus and Magellan Telescopes

Harland W. Epps
The Observatories
Carnegie Institution of Washington
Pasadena, California

May 6, 1989
No. 10

CONTENTS

Abstract

Two possible 315-inch f/1.2 to f/15.0 infrared Cassegrain models are compared by geometric ray trace and diffraction analysis over a 10.0-arcmin diameter field of view. Each has an optimum field curvature and optimum focus to produce maximum energy concentration in its images, averaged over the full field. The main difference between the configurations is that one has an hyperbolic (R/C) primary mirror corrected for zero 3rd order transverse coma while the other has a parabolic (DLS) primary mirror.

Geometric spot diagrams and comparisons of tangential optical path difference (OPD) cuts across the respective exit pupils seem to suggest that the imaging performance of the (R/C) model might be better than the (DLS) model at field angles greater than about 2 arcmin. However, the rms OPD difference between these models does not exceed 0.06 microns at any field location, which is only 0.03 waves (!) at a wavelength of 2.0 microns, and even less over the remainder of the thermal infrared passband.

Diffraction analysis confirms that encircled energy image diameters do not differ between models by more than a few hundredths of an arcsec anywhere in the field of view. In practice such small effects would be completely overwhelmed by seeing and other practical factors such that either model is acceptable and indistinguishable from the other in terms of expected real infrared imaging performance.

It is recommended that the parabolic primary mirror (DLS) model be selected because of the opportunities it affords for unique scientific as well as engineering data taking at an aberrationless prime focus.

1. Introduction

The baseline Columbus Telescope (UA-88-12, July 8, 1988) proposes an f/15 Cassegrain infrared focus with a 10-arcmin diameter curved f.o.v., located some 80 inches behind the primary-mirror vertex. The Airy disk for an aberrationless, unobstructed 315-inch diameter converging wavefront is only 0.13 arcsec in diameter at a wavelength of 2.0 microns, which may be comparable to the seeing under the most ideal conditions. Therefore it is highly desirable to have a "diffraction limited" infrared telescope design.

In a previous report (Epps, January 1989) two possible models containing hyperbolic (R/C) and parabolic (DLS) primary mirrors were compared. It was concluded that rms pathlength errors in these models were comparable through the (DLS) model seemed to be slightly more favorable. The parabolic (DLS) model was recommended because of the opportunity it affords to implement a naked prime focus for scientific purposes and because it would be highly desirable to be able to conduct engineering studies of the primary mirror support system and ventilation/thermal control system as they operate at the telescope. This would best be done by mounting a shearing interferometer at a (potentially) aberration-free prime focus without need of additional optics. There appeared to be no penalty whatever in choosing the parabolic primary mirror, hence that recommendation was made in the January 1989 report.

A more complete study of these alternatives has revealed that by increasing the field curvature some 0.80% and refocusing, it is possible to improve the (R/C) model very slightly while no such improvement appears possible in the (DLS) model. This result reopens the question of whether or not an appreciable difference in infrared imaging performance exists between the optimum (R/C) and (DLS) models.

A full diffraction analysis is required to answer this question quantitatively. The analysis was performed in collaboration with Mr. David Warren of the Aerospace Corporation, using a commercial software package called Code V which is marketed by Optical Research Associates of Pasadena, California. The purposes of this report are to document the results of that diffraction analysis, to summarize conclusions and to make a recommendation regarding the choice of primary mirror conic constant for the Columbus and Magellan telescopes.

2. Geometric Image Analysis for Optimum (R/C) and (DLS) Models

The (new) best (R/C) model is Run No. 6681 (4/24/89) whose system prescription is shown in Table 1. It contains an hyperbolic primary mirror (A_2 = -1.0012621) chosen for zero 3rd order transverse coma. The best (DLS) model is Run No. 7448 (1/20/89) whose system prescription is shown in Table 2. It contains a parabolic primary mirror.

The geometric spot diagrams for the (R/C) model are shown to scale at field angles (0.0, 3.0, 4.0, 5.0) arcmin in Figure 1. They exhibit very slight defocus in the field center and expected 3rd order astigmatism which is the remaining dominant geometric aberration on the optimally curved and focused field of view. Since these images are comparable in size to the (aberrationless) Airy disk at wavelengths of 2 microns or greater, diffraction is obviously important.

The corresponding geometric spot diagrams for the (DLS) model are shown in Figure 2 to the same scale. They exhibit uncorrected 3rd order transverse coma which masks the astigmatism present. It is clear that the geometric ray concentration is less in the (DLS) model along the tangential (vertical) fan, however diffraction effects in the infrared will dominate these images also. Therefore it would not be appropriate to make a quantitative comparison between the (R/C) and (DLS) models on the basis of these geometric data.

3. Diffraction Analysis of Optical Systems in Practice

Diffraction theory is usually approximated in its practical application to the evaluation of imaging performance in optical systems whose typical pathlength errors are less than a few waves; whose f/ratios are larger than about f/3; whose characteristic internal angles near the focal surface are a small fraction of a radian; and where pupil distortion, nontelecentricity and other complications are negligible. For this purpose rays from an object point are traced through the system to an hypothetical reference sphere whose surface passes through the center of the exit pupil and whose center of curvature is located at that point where the chief ray pierces the focal surface. The optical path length of the chief ray, integrated from the entrance pupil to

the reference sphere is subtracted from the corresponding optical path length of every other ray in the bundle such that a unique grid of optical path differences (OPD) at the exit pupil is associated with each point in object space.

It can be shown that the monochromatic diffraction image corresponding to a given object point is approximated by the Fourier transform of its (OPD) distribution over the exit pupil, provided the aforementioned assumptions are not badly violated (see for example: Born and Wolf, *Principles of Optics*, Third (Revised) Edition, Pergamon Press 1965, chapters VIII and IX). As a further approximation, "fast" Fourier transforms (FFT) are often used and the numerical integrals are executed on a finite mesh.

In practice the commercial Code V software is said to be based on mathematical formalism by H. H. Hopkins and M. J. Yzuel (Optica Acta, 1970, Vol. 17, No. 3, pp. 157-182) and by H. H. Hopkins (Applied Optics and Optical Engineering, Vol. IX, Academic Press Inc., 1983, chapter 8). However the Code V source code is highly proprietary and it is not open to objective review and analysis by "outsiders" such as the author and his colleague Mr. Warren.

4. Optical Path Difference (OPD) Analysis for Optimum (R/C) and (DLS) Models

The tangential and sagittal (OPD) distributions across the exit pupil are shown for the (R/C) model in Figure 3 as a function of field angle. It can be seen that the tangential cut shows less than 0.3 microns of maximum aberration amplitude at the 5.0-arcmin field edge while the sagittal cut shows a maximum amplitude of about 1.3 microns.

The corresponding tangential and sagittal (OPD) cuts for the (DLS) model are shown in Figure 4. While the sagittal cuts are nearly identical to those in the (R/C) model, the tangential cut shows a maximum aberration amplitude of about 3.4 microns at the 5.0-arcmin field angle. Its asymmetric shape is characteristic of (known) uncorrected 3rd order transverse coma.

A two-dimensional contour map of (OPD) at the exit pupil for the maximum 5.0-arcmin field angle is shown in Figure 5 for the (R/C) model. Its saddle shape is characteristic of astigmatism. The corresponding worst-case exit pupil map for the (DLS) model is shown in Figure 6. Its shape is characteristic of 3rd order transverse coma and the diagrams confirm that the (DLS) model has a maximum aberration amplitude more than twice as great as that of the (R/C) model.

However the differences are not nearly as much as it might seem. If one calculates the area-weighted rms value of (OPD) over each of the exit pupils the following results are obtained:

field radius (arcmin)	rms (OPD) (microns) (R/C)	(DLS)
on axis	.02	.04
3.0	.13	.18
4.0	.22	.28
5.0	.35	.40

It should be noted that this table cannot be compared exactly with the corresponding table on page 2 in the (Epps, January 1989) report. This is because rms pathlength error is given in the latter reference. Pathlength errors are integrated from the entrance pupil to the detector and thus differ from (OPD) by a large additive constant plus a second order term in those cases where aberration is not zero. Advantages gained by using pathlength error instead of (OPD) involve details of optimization theory that are beyond the scope of this report.

In any case the preceding table suggests that the actual diffraction images for the (R/C) and (DLS) models will not differ by significant amounts due to the fact that the largest rms (OPD) difference seen is only 0.03 waves (!) at a wavelength of 2.0 microns and even less over the remainder of the thermal infrared passband.

5. Integrated Point Spread Function Diffraction Images

The data presented in section 4 were used to calculate integrated point spread function diffraction images for the (R/C) and (DLS) models by the approximate methods described in section 3. A 40-inch diameter central hole was assumed in each of the primary mirrors. The encircled energy in the diffraction images at a wavelength of 2.0 microns is shown at field angles (0.0, 3.0, 4.0, 5.0) arcmin for the R/C model in Figure 7. Image diameters are given in inches at the focal surface. The telescope scale is 0.0229 inches per arcsec which converts to the (awkward) graphical scale of 14.6 inches on the figure per arcsec in the telescope focal surface. The results cannot be considered reliable beyond perhaps 90% encircled energy as can be seen by the fact that the curve shown for the 5.0-arcmin field angle is not even monotonic! However the general shapes of the curves appear to be reasonable.

The corresponding encircled energy in the diffraction images for the (DLS) model is shown at a wavelength of 2.0 microns in Figure 8. Unfortunately an uncontrollable parameter in the software caused these curves to be plotted at a 13.4 inch per arcsec scale which differs from that shown for the (R/C) model in Figure 7. Nevertheless, the represented diffraction images can be compared meaningfully, if carefully (!), up to a limiting encircled energy of perhaps 90%, but certainly not beyond.

Direct numerical data from computer runs at wavelengths of 2.0 microns and 2.5 microns are shown in Table 3 for the (R/C) and (DLS) models. These data include computed diffraction image diameters in arcsec corresponding to (70%, 80%, 90%) encircled energy.

6. Discussion and Conclusions

It can be seen in Table 3 that out to a field radius of about 4.0 arcmin there is certainly no meaningful difference between the computed diffraction imaging performance of the (R/C) and (DLS) models, even at the 2.0-micron short-wavelength limit. It could perhaps be argued that in the field region between 4.0 arcmin and 5.0 arcmin there is a small energy concentration advantage in the (R/C) model which might be seen in practice if the optics were perfectly constructed, aligned, thermalized and supported, and with no atmosphere present.

But one must emphasize that the 90% energy diameters are suspect as discussed in section 5, and there will always be atmospheric seeing and other imperfections which will tend to overwhelm the minute numerical differences seen in Table 3. To a very high degree of practical approximation the (R/C) and (DLS) models appear to be virtually identical with regard to their expected imaging performance in the infrared. This becomes increasingly true as one passes beyond wavelengths near 2.5 microns into the remainder of the thermal infrared passband.

In view of the above quantitative result it can be stated with authority that the choice of primary mirror conic constant between the (R/C) and (DLS) alternatives should not be made on the basis of expected infrared imaging performance over a 10.0-arcmin diameter field of view.

Additionally, it would be very undesirable to adopt an hyperbolic primary mirror for two reasons. The first is that it would foreclose the possibility of very deep coronagraphic ccd imaging over the 10-arcsec diameter f.o.v. in which 0.5-arcsec or better images would be available at parabolic prime focus with an absolute minimum number of optical surfaces in the beam. Suitable targets would be faint companions near bright stars, jet and fuzz near QSOs and AGN; low surface brightness knots and bridges; distant galaxies for morphology, etc. The second equally important reason is that it will be extremely desirable to mount a shearing interferometer directly at prime focus for the purpose of studying the effects of the mirror support system and the ventilation/thermal control system on the primary mirror figure and this is best done at a (potentially) aberration-free image, without additional optics.

For these reasons, it is strongly recommended that a strictly parabolic primary mirror geometry be adopted for the Columbus and Magellan telescopes.

Respectfully submitted,

Harland W. Epps, Ph.D.
Consultant in Optical Design

Acknowledgements

The author wishes to thank Mr. David Warren of the Aerospace Corporation for his valuable insights and expert execution of the calculations presented in this report, using the Code V software licensed to the Aerospace Corporation by Optical Research Associates of Pasadena, California. He also wishes to thank Mr. Darryl E. Gustafson, Senior Vice President, and Mr. Matthew P. Rimmer, Director of Optical Software Development at Optical Research Associates for their generous cooperation in describing and confirming the internal procedures employed in the Code V software to calculate diffraction-related quantities.

APPENDIX

A. Referenced Tables

1. System Prescription: Optimized f/15.0 (R/C) Run No. 6681 (04/24/89)
2. System Prescription: Optimized f/15.0 (DLS) Run No. 7448 (01/20/89)
3. Encircled Energy Diffraction Image Diameter for (R/C) and (DLS) Models

B. Referenced Figures

1. Geometric Spot Diagram Images for (R/C) Model
2. Geometric Spot Diagram Images for (DLS) Model
3. Tangential and Sagittal (OPD) for (R/C) Model
4. Tangential and Sagittal (OPD) for (DLS) Model
5. 5.0-Arcmin Field Angle (OPD) Contour Map for (R/C) Model
6. 5.0-Arcmin Field Angle (OPD) Contour Map for (DLS) Model
7. Integrated Point Spread Function Diffraction Images for (R/C) Model
8. Integrated Point Spread Function Diffraction Images for (DLS) Model

OPTICAL ANALYSIS RUN----PROGRAM OARSA(01/11/89 VERSION)----EPPS/ASTRONOMY/UCLA

Table 1

RN* 2 315-INCH F1.2 - F15.0 IR TELESCOPE MODEL02 (R/C WITH BEST CV-FIELD) RUN NO. 6681 (04/24/89)

FINAL SYSTEM: SCALED TO DABS(GAUSSIAN FOCAL LENGTH)= 4725.000 INCHES RMS IMAGE(S) TYP DIAM= 51.4 +/- 19.5 MICRONS
OBJECT DISTANCE= INFINITY 0.09 +/- 0.03 ARC SEC
APERTURE RADIUS= 157.50 INCHES FIELD RADIUS= 5.00 ARC MIN

CLR DIA	SAG	ASPH	NS	NNE,CRV, 5ASC,NNA NSE,X,4RN,2ICR,NSA	ALL REFLECTING							NS
			1	0								0 1
315.000	0.0	0.0	1	3 -0.38336394D+04	0.10000000D+01	0.0	0.10000000D+01	0.0		0	0	0 1
			2	3 -0.13227535D-02	-0.10012621D+01	0.0	0.0	0.0	0.0			0 2
327.898	-17.777	0.0525	2	8 -0.34407349D+03	-0.10000000D+01	0.0	-0.10000000D+01	0.0		0	0	0 2
			3	3 -0.13558975D-01	-0.13961305D+01	0.0	0.0	0.0	0.0			0 3
28.543	-1.376	0.0045	3	9 0.42407413D+03	0.10000000D+01	0.0	0.10000000D+01	0.0		0	0	0 3
			4	90 -0.30078291D-01	0.0	-0.223692690-02	-0.52686082D-02	-0.10281673D-01	0.0		-1	4
13.725	-0.716	0.0	4	2 0.24895094D-03	0.10000000D+01	0.0	0.10000000D+01	0.0		0	0	0 4

NOTICE: END OF COMPUTATIONS FOR THIS SYSTEM. TERMINATION WAS NORMAL.

OPTICAL OPTIMIZATION RUN----PROGRAM OARSA(01/11/89 VERSION)----EPPS/ASTRONOMY/UCLA

Table 2

RN* 2 315-INCH F1.2 - F15.0 IR TELESCOPE MODEL01 (DLS WITH BEST CV-FIELD) RUN NO. 7448 (01/20/89)

FINAL SYSTEM: SCALED TO DABS(GAUSSIAN FOCAL LENGTH)= 4725.000 INCHES
OBJECT DISTANCE= INFINITY
APERTURE RADIUS= 157.50 INCHES FIELD RADIUS= 5.00 ARC MIN

RMS IMAGE(S) TYP DIAM= 85.1 +/- 25.6 MICRONS
0.15 +/- 0.04 ARC SEC

CLR DIA	SAG	ASPH	NS	NNE,CRV, 5ASC,NNA NSE,X,4RN,2ICR,NSA	ALL REFLECTING								NS
			1	0								0	1
315.000	0.0	0.0	1	3 -0.38327542D+04	0.10000000D+01	0.0	0.10000000D+01	0.0		0	0	0	1
			2	3 -0.13227543D-02	-0.10000000D+01	0.0	0.0	0.0	0.0			0	2
327.895	-17.777	0.0525	2	8 -0.34406619D+03	-0.10000000D+01	0.0	-0.10000000D+01	0.0		0	0	0	2
			3	3 -0.13556140D-01	-0.13780718D+01	-0.10047033D-09	-0.54506368D-13	0.0	0.0			0	3
28.542	-1.376	0.0044	3	9 0.42416306D+03	0.10000000D+01	0.0	0.10000000D+01	0.0		0	0	0	3
			4	90 -0.29576863D-01	0.0	-0.20213119D-02	-0.40564993D-02	-0.81008688D-02	0.0			-1	4
13.736	-0.705	0.0	4	2 0.69565911D-02	0.10000000D+01	0.0	0.10000000D+01	0.0		0	0	0	4

NOTICE: END OF COMPUTATIONS FOR THIS SYSTEM. TERMINATION WAS NORMAL.

Table 3. Encircled Energy Diffraction Image Diameter (Arcsec) For (R/C) and (DLS) Models

1. New (R/C) Run No. 6681 (4/24/89) 315-inch f/1.2 to f/15.0 infrared baseline model

Wavelength = 2.0 microns

(Energy)	f.a. = 0.0	3.0 arcmin	4.0 arcmin	5.0 arcmin
70%	.08	.10	.13	.17
80%	.15	.16	.17	.22
90%	.21	.25	.27	.31

Wavelength = 2.5 microns

(Energy)	f.a. = 0.0	3.0 arcmin	4.0 arcmin	5.0 arcmin
70%	.10	.11	.14	.19
80%	.18	.19	.20	.24
90%	.27	.29	.33	.36

2. Old (DLS) Run No. 7448 (1/20/89) 315-inch f/1.2 to f/15.0 infrared baseline model

Wavelength = 2.0 microns

(Energy)	f.a. = 0.0	3.0 arcmin	4.0 arcmin	5.0 arcmin
70%	.08	.13	.16	.21
80%	.15	.17	.21	.27
90%	.22	.30	.33	.39

Wavelength = 2.5 microns

(Energy)	f.a. = 0.0	3.0 arcmin	4.0 arcmin	5.0 arcmin
70%	.10	.15	.18	.22
80%	.19	.20	.22	.29
90%	.27	.35	.37	.44

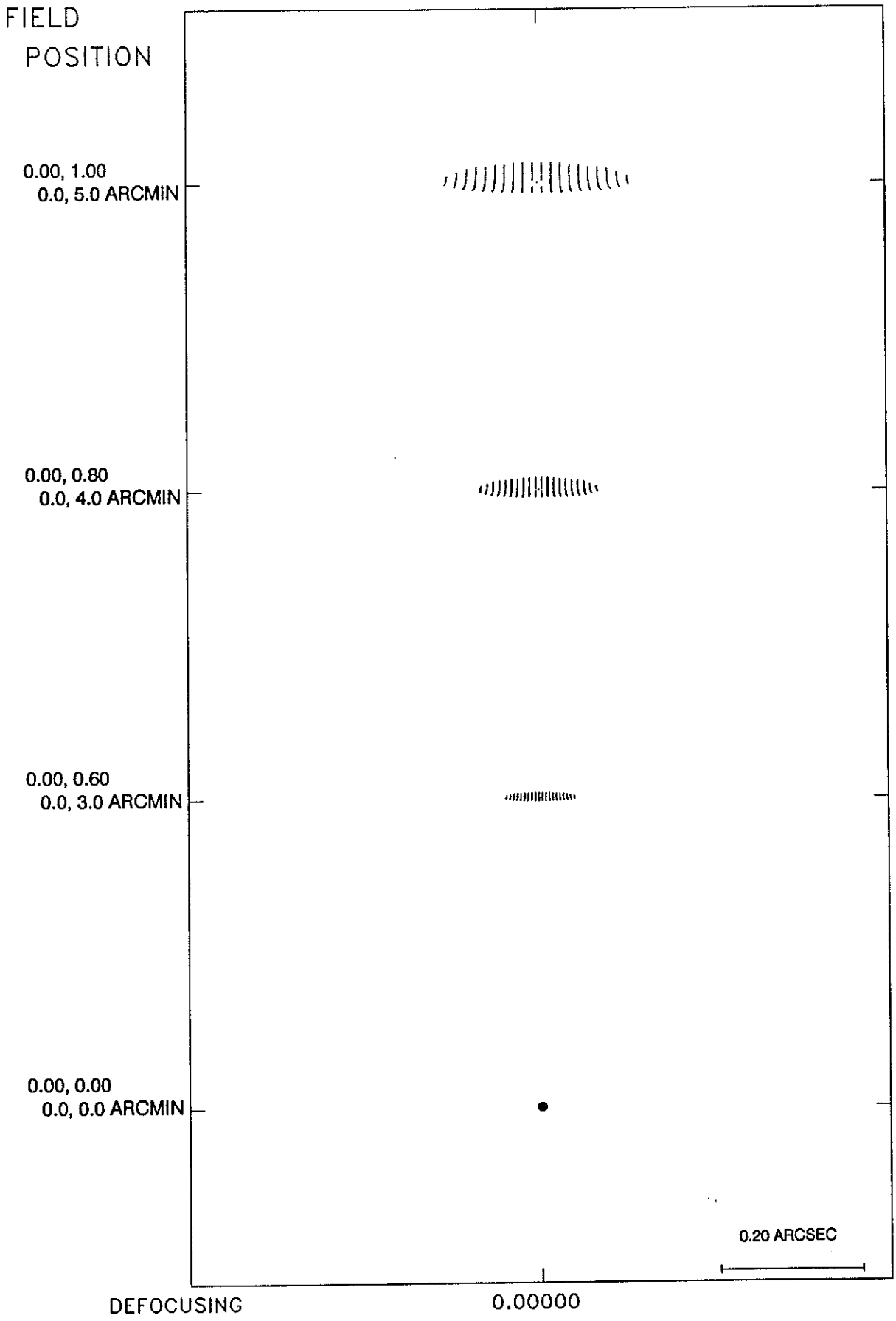
FIELD
POSITION
0.00, 1.00
0.0, 5.0 ARCMIN
0.00, 0.80
0.0, 4.0 ARCMIN
0.00, 0.60
0.0, 3.0 ARCMIN
0.00, 0.00
0.0, 0.0 ARCMIN
0.20 ARCSEC
DEFOCUSING
0.00000
R/C #6681 (4/24/89)

Figure 1

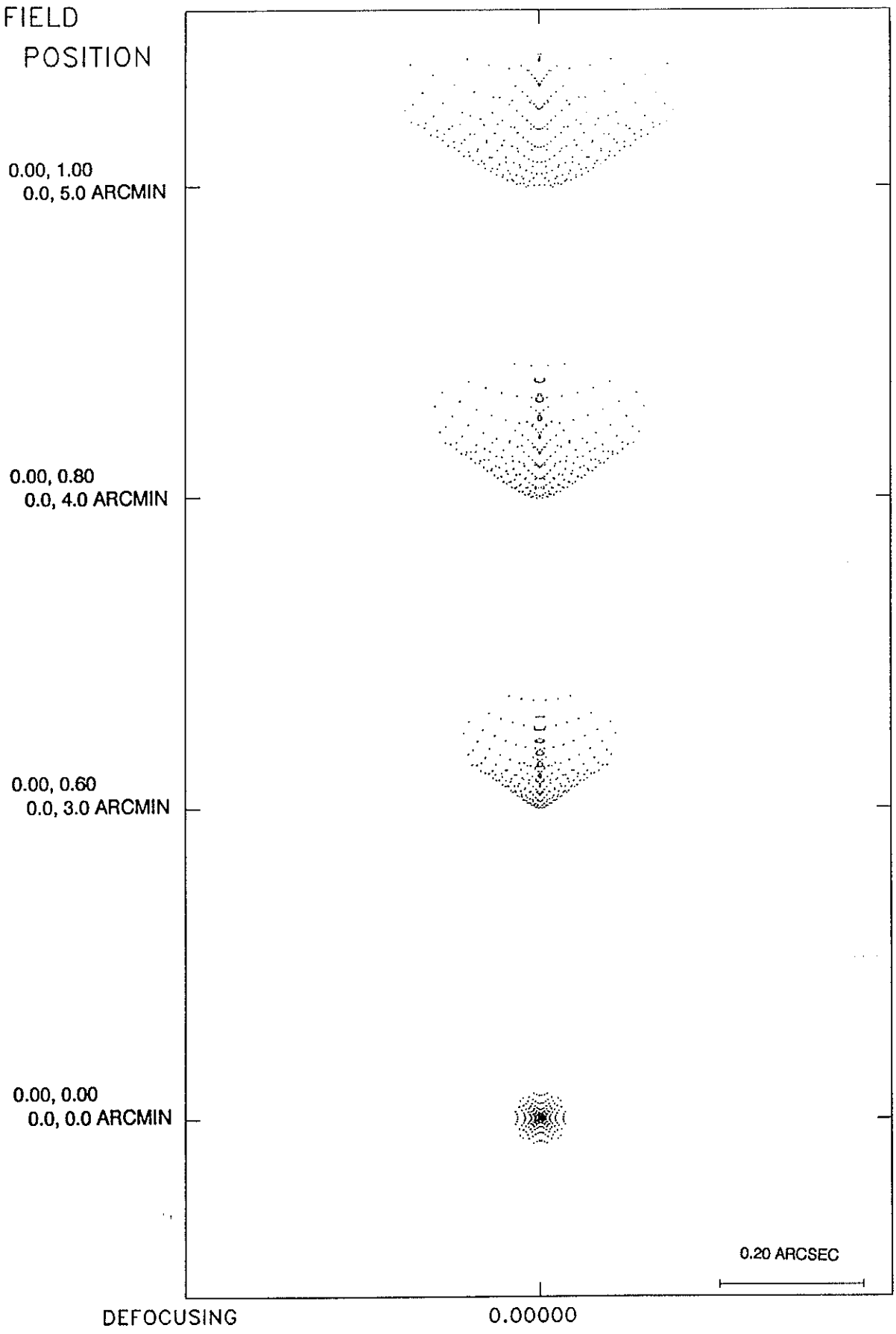
FIELD
POSITION
0.00, 1.00
0.0, 5.0 ARCMIN
0.00, 0.80
0.0, 4.0 ARCMIN
0.00, 0.60
0.0, 3.0 ARCMIN
0.00, 0.00
0.0, 0.0 ARCMIN
0.20 ARCSEC
DEFOCUSING
0.00000
DLS #7448 (1/20/89)

Figure 2

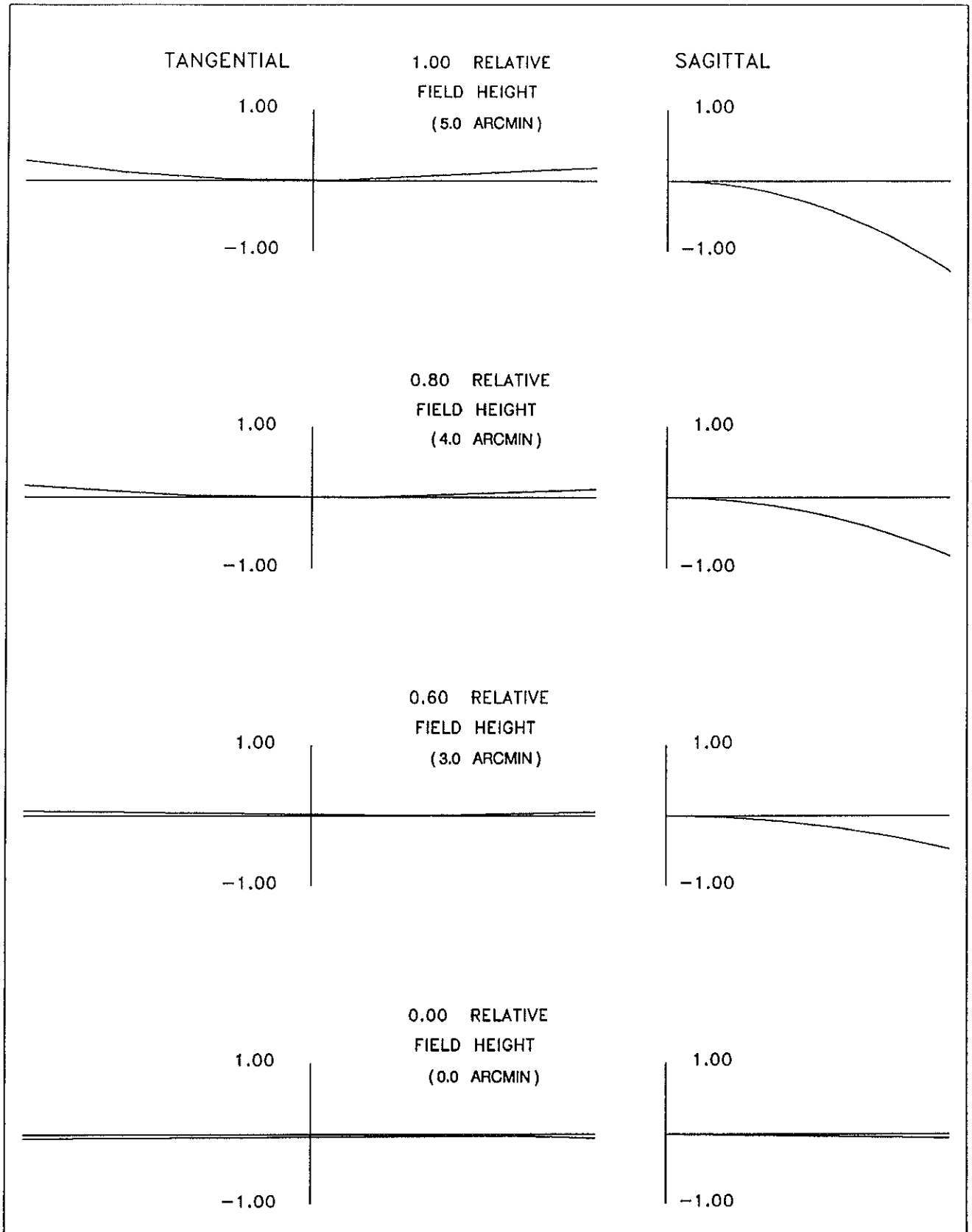

R/C #6681 (4/24/89)

OPTICAL PATH DIFFERENCE (MICRONS)

3−MAY−89

2.0 MICRONS

Figure 3

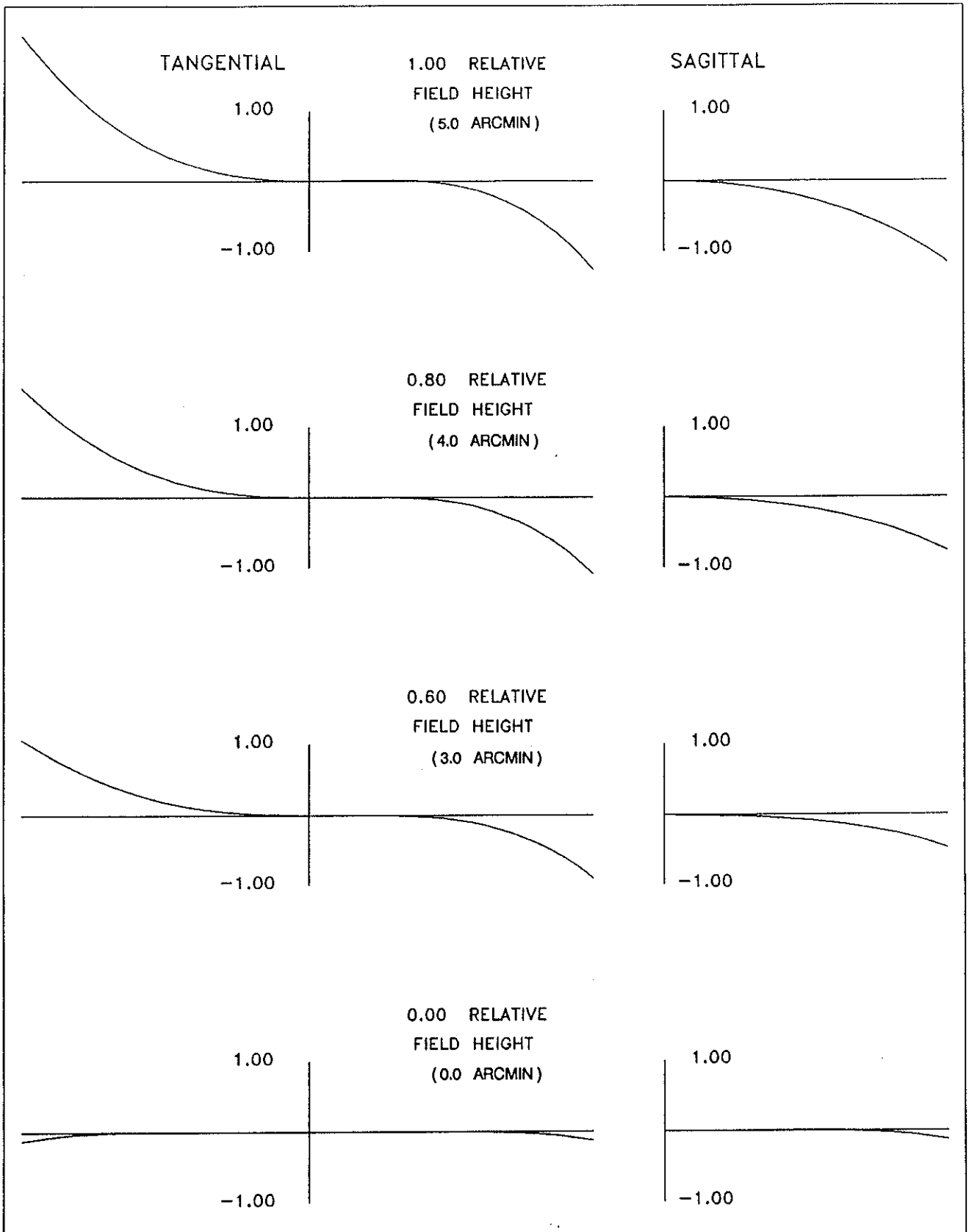

DLS #7448 (1/20/89)

OPTICAL PATH DIFFERENCE (MICRONS)

3-MAY-89

2.0 MICRONS

Figure 4

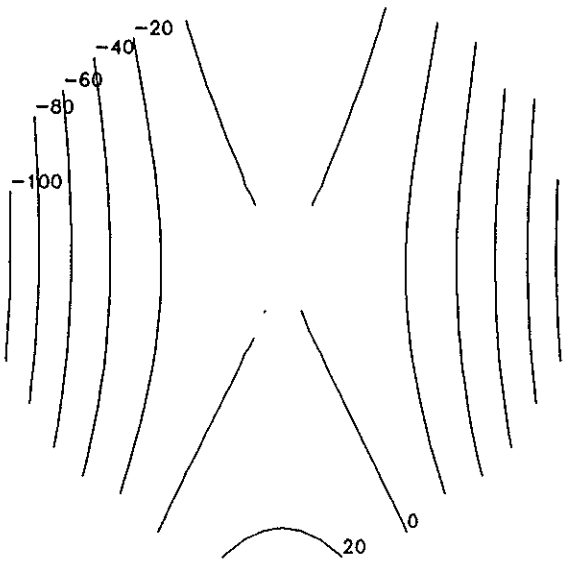

R/C #6681 (4/24/89)

EXIT PUPIL (OPD) MAP
(WAVEFRONT ABERRATION)

3-MAY-89

FLD(0.00, 1.00)MAX,(0.0, 5.0)ARCMIN

DEFOCUSING 0.000000 IN.

CONTOUR INTERVAL 0.20 MICRONS

MIN/MAX: -1.28 / 0.25 MICRONS

Figure 5

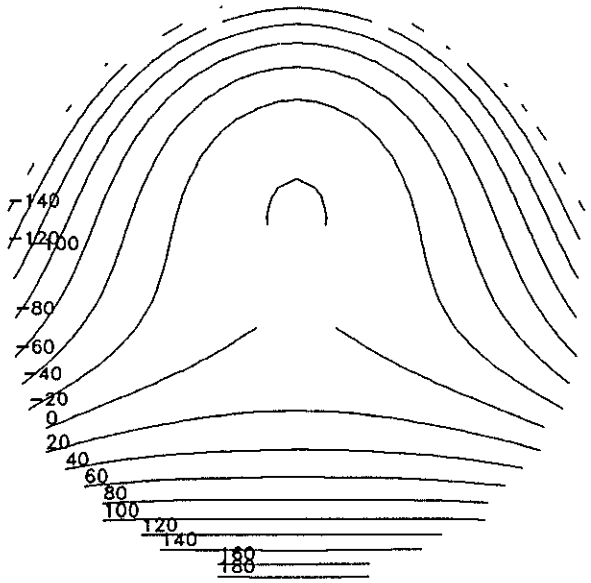

DLS #7448 (1/20/89)

EXIT PUPIL (OPD) MAP
(WAVEFRONT ABERRATION)

3-MAY-89

FLD(0.00, 1.00)MAX,(0.0, 5.0)ARCMIN

DEFOCUSING 0.000000 IN.

CONTOUR INTERVAL 0.20 MICRONS

MIN/MAX: -1.56 / 1.85 MICRONS

Figure 6

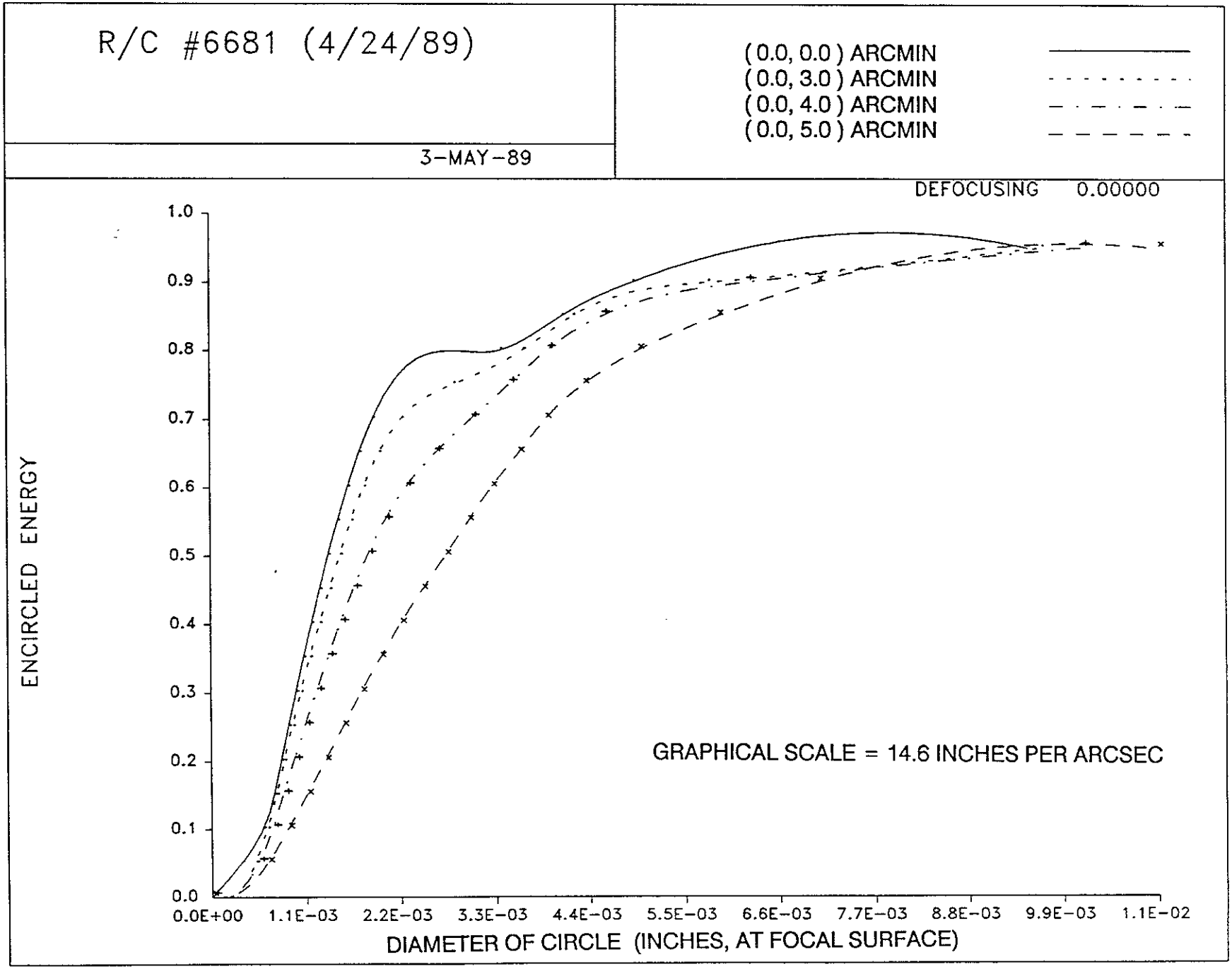
R/C #6681 (4/24/89)
3-MAY-89
(0.0, 0.0) ARCMIN
(0.0, 3.0) ARCMIN
(0.0, 4.0) ARCMIN
(0.0, 5.0) ARCMIN
DEFOCUSING 0.00000
ENCIRCLED ENERGY
1.0
0.9
0.8
0.7
0.6
0.5
0.4
0.3
0.2
0.1
0.0
0.0E+00
1.1E-03
2.2E-03
3.3E-03
4.4E-03
5.5E-03
6.6E-03
7.7E-03
8.8E-03
9.9E-03
1.1E-02
DIAMETER OF CIRCLE (INCHES, AT FOCAL SURFACE)
GRAPHICAL SCALE = 14.6 INCHES PER ARCSEC

Figure 7

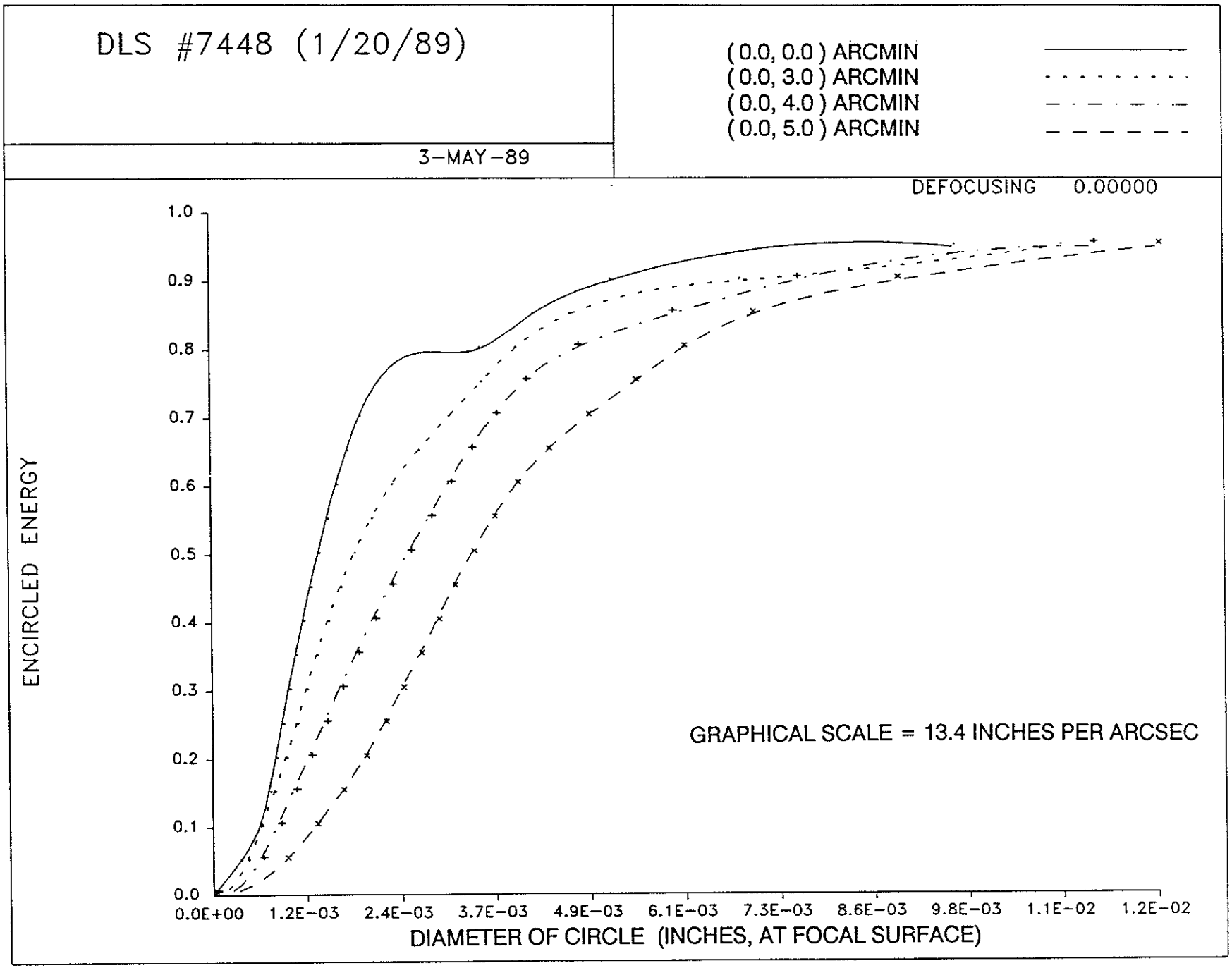
DLS #7448 (1/20/89)
3-MAY-89
(0.0, 0.0) ARCMIN
(0.0, 3.0) ARCMIN
(0.0, 4.0) ARCMIN
(0.0, 5.0) ARCMIN
DEFOCUSING 0.00000
ENCIRCLED ENERGY
1.0
0.9
0.8
0.7
0.6
0.5
0.4
0.3
0.2
0.1
0.0
GRAPHICAL SCALE = 13.4 INCHES PER ARCSEC
0.0E+00
1.2E-03
2.4E-03
3.7E-03
4.9E-03
6.1E-03
7.3E-03
8.6E-03
9.8E-03
1.1E-02
1.2E-02
DIAMETER OF CIRCLE (INCHES, AT FOCAL SURFACE)

Figure 8